ESR studies of stearic acid binding to bovine serum albumin

Mingtao Ge, Shankar B. Rananavare * and Jack H. Freed

Baker Laboratory of Chemistry, Cornell University, Ithaca, NY (U.S.A.)

The ESR spectra of a series of chain-labelled doxyl stearic acids (5-, 7-, 12- and 16-DSA) and doxyl methyl stearates (5-, 7-, 12- and 16-DMS) bound to the high-affinity binding sites of bovine serum albumin (BSA) have been analyzed using nonlinear least-squares fitting of slow-motional ESR simulation. The motional analysis reveals that the rotational diffusion of these stearates around the axis perpendicular to the long hydrocarbon chain is greatly hindered, suggesting that they are held tightly in a channel of the protein. Comparison of the isotropic hyperfine splitting, A_0, among each series shows that 5- and 16-DSA and 16-DMS have larger A_0 values than the other spin labels. In addition, labels at the 16-C position of both DSA and DMS exhibit significantly increased motion relative to the other positions. These observations suggest that the channel starts at 5-C of the chain and ends somewhere between 13-C and 15-C, leading to an estimate of 11 ± 1 Å for the length of the channel. The methyl stearate labels exhibit significantly faster rotation around the chain axis than the analogous stearic acid labels, suggesting a double hydrogen-bonding mechanism for fatty acid binding to BSA. The ability of the acid to form two hydrogen bonds apparently fixes it more rigidly in the protein, preventing rotation about either single hydrogen bond. A double-hydrogen bonding mechanism is most consistent with the formation of a salt bridge between the negatively charged carboxylate of the acid and either a positively charged guanidino group of arginine, or the positively charged ω-amino groups of two lysine residues. An ESR study of the pH dependence of DSA binding indicates that salt bridge formation with lysine is responsible for at least some of the long chain fatty acid binding sites of BSA.

Introduction

Due to its remarkable ability for ligand binding and its important role in transporting fatty acid in the blood, albumin has been one of the most extensively studied proteins. Various experimental approaches have been utilized to study long-chain fatty acid binding to BSA including fluorescence measurements [1–4], partition analysis [5–11], chemical modification [12,13], NMR [14–19] and other spectroscopic methods [20,21]. The spin-label technique has also been used for measur-

ing the equilibrium binding constants [22], probing the binding sites, and monitoring the molecular motion of bound fatty acid [2,3,21,23–27]. Based on the observed interaction of arginine with doxyl stearate, Wallach and co-workers [21] concluded that arginine is responsible for the binding of stearic acid. An analysis of aldehyde modification of arginine in BSA by Jonas and Weber [12] also suggested that there are arginine residues at or close to the strong hydrophobic binding sites of BSA.

More recently a three-dimensional model of albumin structure has been proposed by Brown and Shockley (BS) [28]. This model consists of three domains, each of which has a hydrophobic channel running through the center; each domain in turn contains two subdomains formed by three α-helices. The positively charged amino acid residues located at the opposite ends of each domain are responsible for fatty acid binding via electrostatic bonds with the fatty carboxyl group, thus creating six long-chain fatty acid binding sites. Brown and Shockley suggested that the subdomains 1-C, 2-C and 3-C correspond to the primary long-chain fatty acid binding sites. By correlating the BS model with ^{13}C-NMR data of ^{13}C enriched fatty acids bound to BSA,

---

* Present address: Department of Chemical and Biological Science, Oregon Graduate Institute, 19600 NW Von Neumann Drive, Beaverton, OR, 97006-19999,U.S.A.

Abbreviations: BSA, bovine serum albumin; DSA, doxyl stearic acid; DMS, doxyl methyl stearate; DAZ, *N*-dansylaziridine; BS, Brown and Shockley, Ref. 28.

Correspondence: J.H. Freed, Department of Chemistry, Baker Laboratory, Cornell University, Ithaca, NY 14853, U.S.A.

Cistola et al. [17,18] identified three high-affinity binding sites in the protein, and assigned them to the Lys-His-Lys cluster in subdomain 3-C and to the His-Arg-Arg clusters in subdomains 1-C and 2-C.

However, discrepancies with regard to the binding site for long-chain fatty acids remain. For example, in a phosphorescence and optically detected magnetic resonance study, Mao and Maki [14] shows that Trp-134 in BSA was the primary binding site of long-chain fatty acids. Based on the ^{1}H-NMR study on the interaction of human serum albumin with fatty acid, Oida [15] suggested that histidine, tyrosine and lysine residues are involved in the primary fatty acid binding.

The striking capacity of albumin for binding fatty acids has been known for a long time [29]. Several studies have indicated that there are only six high-affinity binding sites for long-chain fatty acids [6,8,17,18], consistent with the model of Brown and Shockley [28].

It is well known that slow-motional ESR spectra of nitroxide radicals are very sensitive to changes in their molecular dynamics as well as variations in the polarity of their surroundings. Previous ESR studies of fatty acid binding to BSA have relied on the splitting of the outer peaks in the spectrum as a crude measure of spin-label mobility [2], or have utilized paramagnetic line-broadening agents to estimate the exposure of spin labels to solvent [26]. However, recent advances in the computational efficiency of slow-motional ESR spectral simulation [31,32] have permitted the application of high accurate nonlinear least-squares methods for fitting experimental slow-motional spectra [46]. The aim of the present study is to demonstrate how detailed and quantitative analysis of spin probe motion can serve to further characterize fatty acids binding to BSA.

We have used our nonlinear least-squares program to make a careful interpretation of ESR spectra from 5-, 7-, 12- and 16-DSA and DMS spin labels bound to one of the long-chain fatty acid high affinity binding sites of BSA. The analysis reveals new details of the motions of fatty acids bound to the high-affinity binding sites of BSA. Specifically, the motional parameters depend on the position of the moiety of the nitroxide radical, and can be used to estimate the dimension of the channel in BSA, by analogy with the 'molecular dipstick' method in which spin labels of varying chain length are used to map the topology of an enzymatic active site [30]. The analysis also shows significant differences in the rotational rates of DSA and DMS about their chain axes, suggesting that the acid is bound to the protein by a double-hydrogen bond. These results will be discussed in terms of current models for the fatty acid binding mechanism of BSA. Evidence for salt bridge formation of the fatty acid with the lysine residue will be provided from the pH-dependent study of stearic acid binding to BSA.

Experimental procedures

Crystallized, fatty acid-free BSA was purchased from Sigma Chemicals and used without further purification. The buffer solutions used in this study were 0.05 M potassium biphthalate solution at pH 5; 0.02 M phosphate solution at pH values of 6, 7.4 and 8; 0.05 M borate/potassium chloride solution at pH 9 and 10; and 0.05 M ammonia/ammonium chloride solution at pH 11.

Freshly made solutions of BSA in buffer were kept refrigerated not longer than 24 h before use. 5-, 7-, 12- and 16-doxyl stearic acid were obtained from Aldrich and Molecular Probe and 5-, 7-, 12- and 16-doxyl methyl stearate from Aldrich. The spin probes were kept in chloroform solutions in the freezer.

The albumin samples bound with doxyl stearate were prepared as follows. The correct amount of chloroform solution of doxyl stearate was put into a sample tube, and the solvent removed by flowing nitrogen gas. A measured amount of buffered BSA solution was added to the sample tube, and the solution was stirred for several minutes. The binding was completed within 5 min. 15 μl of the above solution was transferred by microsyringe to a capillary for taking the ESR spectrum. Because of the low solubility of methyl stearate in water, albumin-doxyl methyl stearate solutions were stirred for 12 h.

The critical micelle concentrations of 5- and 7-DSA in pH 7.4 buffer solution were measured to be approx. $1.5 \cdot 10^{-3}$ M and approx. $2.5 \cdot 10^{-3}$ M, respectively. Since 12- and 16-DSA are more soluble than 5- and 7-DSA, they do not form micelles in unsaturated solutions. In all the samples used in this study, the concentration of spin-labelled stearate was $5 \cdot 10^{-4}$ M, well below the measured critical micelle concentrations. The molecular weight of BSA used for calculating the concentration of BSA was taken as 67.5 kDa [33].

The spin labels were bound to BSA in a molar ratio of 1:1 in pH 7.4 buffer solution and their ESR spectra were obtained at 23°C. The ESR spectra were taken on a Bruker ER 200D-SRC spectrometer. The rigid limit spectra of 5-, 7-, 12- and 16-DSA bound to BSA in a molar ratio 1:1 at pH 7.4 were recorded at -30°C using a Bruker VT-1000 variable temperature unit. pH-dependent experimental data include spectra of 12-DSA added to BSA in a molar ratio of 5:1 for pH values of 5–12. When the pH is lower than 5, the solubilities of both BSA and 12-DSA decrease, and BSA precipitates. The number of 12-DSA molecules bound to BSA at molar ratios of 12-DSA/BSA ranging from 2:1 to 25:1 were compared at pH 7.4 and pH 9.0. Spectral subtraction and double integration were used to calculate the concentration of bound vs. unbound spin-labelled stearates.

Results

ESR spectra of 12-DSA added to BSA in the molar ratio of 5 : 1 at various pH values are depicted in Fig. 1. Each spectrum is a superposition of a broad and a narrow component, corresponding to bound and un-bound 12-DSA, respectively. In Fig. 2 the number of 12-DSA molecules bound to BSA is plotted vs. pH. Over the range of pH 5 to 10 there is not much change observed in this number, although a weak maximum value of 5.0 seems to occur at pH 6. However, at pH 11 the number drops to 4.3 and at pH 12 BSA loses its binding ability completely, i.e., denaturation of BSA has occurred. The pH dependence of BSA binding of 12-DSA is also shown in Fig. 3, in which the average number (n) of 12-DSA bound to one BSA is plotted vs. the logarithm of the concentration of unbound 12-DSA at pH values of 7.4 and 9. The value of n decreases from about 13.5 to 7.0 when the pH is increased from 7.4 to 9.0 in the case of a molar ratio of 12-DSA/BSA of 20 : 1. This value of 7 is close to that for the high-affinity binding site of 6, obtained by other investigators [6,8,18,28].

The room temperature (23°C) spectra from 5-, 7-, 12- and 16-DSA and from 5-, 7-, 12- and 16-DMS bound to BSA at pH 7.4 in a 1 : 1 molar ratio were simulated. We achieved good agreement between experimental and simulated spectra, shown in Fig. 4 by using the method of nonlinear least-squares fitting [46]. The best-fit parameters of the nuclear hyperfine tensor components, A_{xx}, A_{yy}, A_{zz}, the rotational diffusion coefficients $R_{\perp}$, $R_{\parallel}$, which are the principal values of

Fig. 2. Plot of the average number of 12-DSA molecules bound to one BSA vs. pH of the solution in a molar ratio of 12-DSA/BSA of 5.

an axially symmetric rotational diffusion tensor [34], and the inhomogeneous line width T_2^{-1*} are listed in Table II. It is known that the hydrodynamic behavior of BSA can be described as that of a prolate ellipsoid [35]. From the transient electric birefringence measurements on BSA given by Wright and Thompson [36], the principal rotation diffusion coefficients around the minor and the major axis are $2.2 \cdot 10^6$ s^{-1} and $8.3 \cdot 10^6$ s^{-1}, respectively. These values are very close to the $R_{\perp}$ values for bound 5-, 7- and 12-DSA and bound 5-, 7- and 12-DMS, showing that the rotational coefficients of these bound stearates about the axis perpendicular to the long hydrocarbon chain are of the same order of magnitude as the tumbling rate of the BSA molecule.

The values of the g tensor components g_{xx}, g_{yy}, g_{zz}, used for the simulations were obtained from simulation of the rigid limit (-30°C) spectra of bound 5-, 7-, 12- and 16-DSA at pH 7.4. The observed and simulated
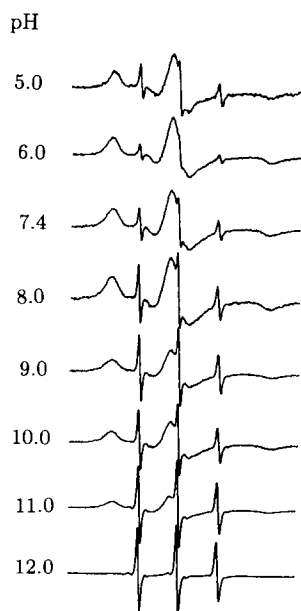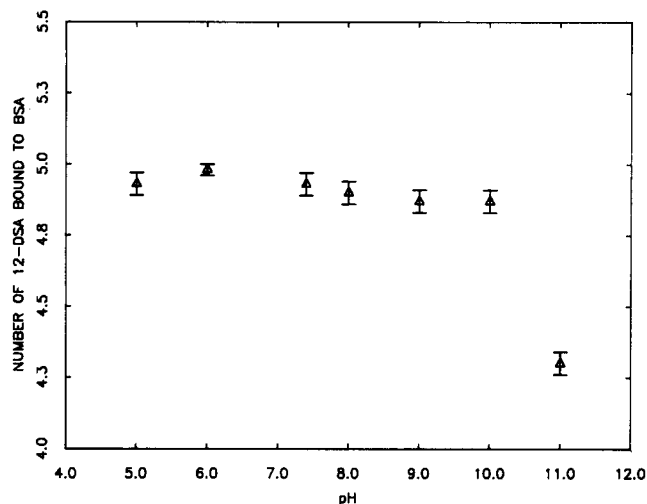
pH

Fig. 1. ESR spectra from 12-DSA bound to BSA in the molar ratio of 5 : 1 at various pH values. The broad and narrow components correspond to bound and unbound 12-DSA, respectively.
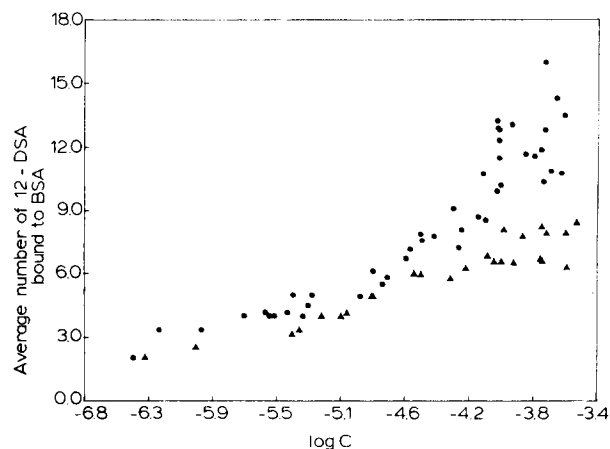

Fig. 3. Plot of the average number of 12-DSA molecules bound to one BSA vs. the logarithm of concentration of unbound 12-DSA at pH 7.4 (●), and pH 9 (▲).
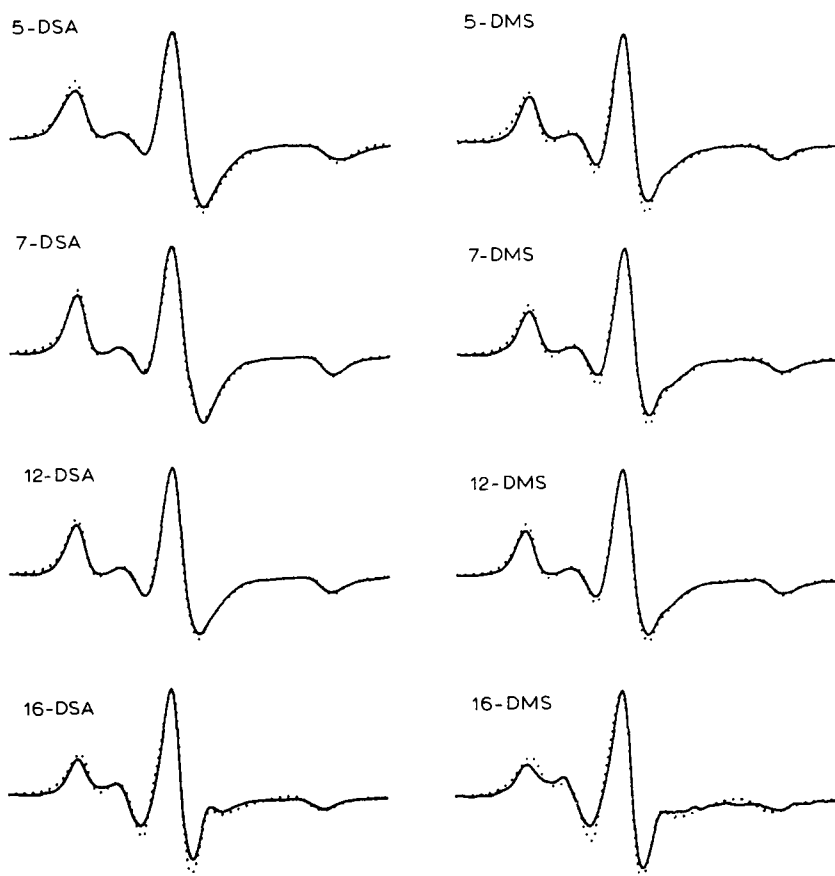
Fig. 4. Experimental (solid line) and simulated (dotted line) ESR spectra from 5-, 7-, 12- and 16-DSA and 5-, 7-, 12- and 16-DMS bound to BSA in the molar ratio of BSA to spin-labelled stearates of 1 : 1 at pH 7.4 and 23°C.

rigid limit ESR spectra are shown in Fig. 5. In all cases the agreement is very good. The best-fit values of the g tensor components from the rigid limit spectra are 2.0086, 2.0063 and 2.0025, respectively, which are consistent with the values obtained by Gaffney and McConnell [37]. The best fit A tensor components of the rigid limit spectra are listed in Table I. We noticed that the values of the A tensor components obtained from the rigid limit spectra were a little different than those from simulation of the room temperature spectra. We attribute these differences to the change of the tertiary structure of BSA when BSA is cooled to $-30°C$. Because the sensitivity of the simulation is not high enough to distinguish the differences between the spectra from different molar ratio of BSA to spin labels, only the simulations of spectra with molar ratio of BSA/doxyl stearate of 1 : 1 were carried out. A simulation of unbound 16-DSA at pH 7.4 was also performed, and the best-fit parameters of $R_\perp$ and $R_\parallel$ and A_0 are also listed in the footnote of Table II.

Discussion

Estimation of dimension of the channel

The difference of rotational diffusion coefficients between bound 5-, 7-, 12- and 16-DSA can be seen from

Table II. The values of $R_\perp$ for bound 5-, 7- and 12-DSA are near the rigid limit and practically the same. The value of $R_\perp$ for bound 16-DSA is faster by a factor of 2.6. In contrast, the $R_\parallel$ values increase from $3 \cdot 10^7$ s^{-1} for bound 5-, 7- and 12-DSA to $1.0 \cdot 10^9$ s^{-1} for bound 16-DSA, i.e., by more than one order of magnitude! The values of $R_\perp$ and $R_\parallel$ show a similar trend in the DMS series. The $R_\perp$ values are comparable (and near rigid limit) for bound 5-, 7- and 12-DMS, but are about 2-2.5-times larger for bound 16-DMS, while the $R_\parallel$ value increases by a factor of 13-16, from approx. $8 \cdot 10^7$ s^{-1} for bound 5-, 7- and 12-DMS to $1.1 \cdot 10^9$ s^{-1} for bound 16-DMS. We also note that both the $R_\perp$ and the $R_\parallel$ values for bound 5-, 7- and 12-DMS are greater than those of bound 5-, 7- and 12-DSA. Considering that the values of $R_\parallel$ for bound DMS are 2.0-2.6-times greater than those for bound DSA, whereas the uncertainties in the best-fit values for $R_\parallel$ and $R_\perp$ are 50 and 20%, respectively, the differences of $R_\perp$ and $R_\parallel$ between the bound DMS and DSA are significant. Differences between the spectra from DMS and DSA were obtained qualitatively by Morrisett et al. [2], who have noted the small but discernible difference in the line shapes between bound DSA and DMS. That is, they found an inflection on the high field side of the center peak of the spectra from bound DMS, whereas
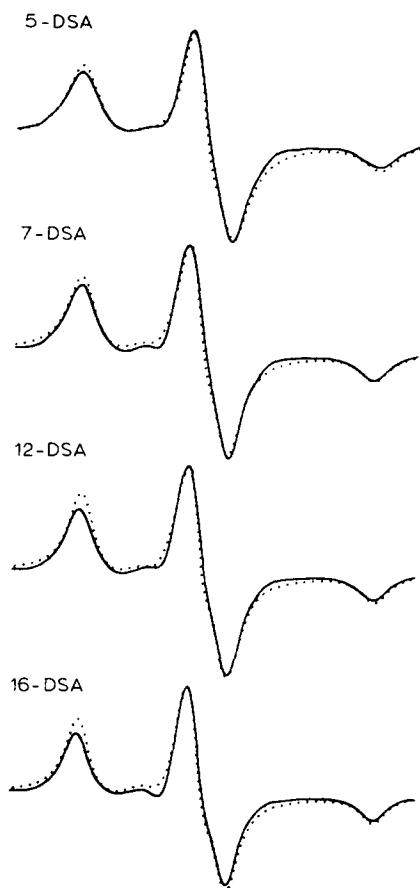
5-DSA

7-DSA

12-DSA

16-DSA

Fig. 5. Experimental (solid line) and simulated (dotted line) rigid limit ESR spectra of 5-, 7-, 12- and 16-DSA bound to BSA in the molar ratio of 1 : 1 at pH 7.4 and $-30\,^{\circ}$C.

this feature is absent in the spectra of bound DSA. We have succeeded in quantifying and identifying the sources of these spectral differences. Accompanying the changes of $R_\perp$ and $R_\parallel$, we found that the A_0 values change from 15.1 gauss for bound 7- and 12-DSA and

TABLE I

A-tensor component from simulation of rigid limit spectra ($-30\,^{\circ}C$) of 5-, 7-, 12- and 16-DSA bound to BSA

	A_{xx}	A_{yy}	A_{zz}	A_0
5-DSA	6.6	5.5	34.5	15.5
7-DSA	6.6	4.8	33.9	15.1
12-DSA	6.6	4.8	33.9	15.1
16-DSA	6.1	5.6	34.2	15.3

Unit = gauss.

bound 5-, 7- and 12-DMS to 15.3 gauss for bound 16-DSA and 16-DMS.

The near rigid limit value of $R_\perp$ and large ratios $N = R_\parallel/R_\perp$, for these bound DSA and DMS indicate that the rotational diffusion of bound stearic acid and methyl stearate around the axis perpendicular to the hydrocarbon chain is greatly hindered, whereas the rotational diffusion around the chain axis is much easier. These characteristics are consistent with the idea that both stearates bound to BSA are trapped in a narrow channel. The variation of A_0, $R_\perp$, and $R_\parallel$ values with the position of the nitroxide radical (Figs. 6, 7) indicates that 7-C and 12-C nitroxide radicals are more tightly trapped inside the hydrophobic channel, but the 16-C nitroxide radicals protrude from the channel and reside in a more polar and less hindered environment, permitting significant degree of internal motion. Since the values of $R_\perp$, $R_\parallel$ and A_0 for 16-DSA and 16-DMS are nearly identical, we propose that DSA and DMS occupy the same binding site or quite similar binding sites in BSA. The closeness of the A_0, $R_\perp$ and $R_\parallel$ values among the 5-, 7- and 12-DMS indicate that the 5-C, 7-C and 12-C doxyl groups in bound methyl stearate have a similar hydrophobic and hindering environment. Although 5-DSA has similar $R_\perp$ and $R_\parallel$ values to 7- and

TABLE II

Parameters from simulation of spectra ($23\,^{\circ}C$) of spin-labelled stearates bound to BSA [a]

	A_{xx}	A_{yy}	A_{zz}	A_0	$R_\perp$	$R_\parallel$	N	T_2^{-1}*
5-DSA	6.9	5.4	33.8	15.4	5.0×10^6	3.6×10^7	7	2.6
7-DSA	6.9	5.4	33.0	15.1	5.0×10^6	3.1×10^7	6	2.2
12-DSA	6.9	5.4	33.0	15.1	4.9×10^6	3.1×10^7	6	1.8
16-DSA	6.7	6.1	33.2	15.3	1.3×10^7	1.0×10^9	77	0.9
5-DMS	6.9	5.4	33.0	15.1	7.5×10^6	7.5×10^7	10	1.7
7-DMS	6.9	5.4	33.0	15.1	7.0×10^6	7.9×10^7	11	1.7
12-DMS	6.9	5.4	33.0	15.1	6.5×10^6	8.2×10^7	13	1.9
16-DMS	6.7	6.0	33.2	15.3	1.6×10^7	1.1×10^9	69	1.2

[a] (i) The best-fit parameters for unbound 16-DSA at pH 7.4: A_0, 15.8 gauss; $R_\perp$, $2.8 \cdot 10^{10}$ s^{-1}, $R_\parallel$, $4.6 \cdot 10^{10}$ s^{-1}, T_2^{-1}*, 0.7 gauss.
(ii) Molar ratio of BSA/DSA or to DMS is 1 : 1. All samples are in pH 7.4 buffer solution.
(iii) Units used: A-tensor components, gauss; A_0, gauss; $R_\perp$, $R_\parallel$, s^{-1}; T_2^{-1}*, gauss.
(iv) $A_0 = (A_{xx} + A_{yy} + A_{zz})/3$.
(v) Estimated errors: $\pm 1\%$ in A_{xx}, A_{yy}, $\pm 0.3\%$ in A_{zz}, $\pm 20\%$ in $R_\perp$, $\pm 50\%$ in $R_\parallel$ $\pm 10\%$ in T_2^{-1}*.
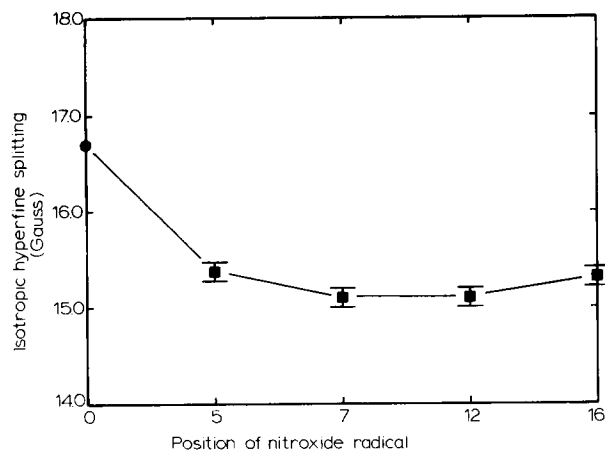
Fig. 6. Plot of isotropic hyperfine splitting A_0 of DSA bound to BSA in the molar ratio of 1:1 vs. position of carbon atom to which the nitroxide moiety is attached. First data point is the A_0 value of the ESR spectrum of (2,2,6,6-tetramethyl-4-oxyl-piperidine)stearate bound to BSA from Kuznetsov et al. [25].

located at the end of the channel. These suggestions are consistent with the order of decrease in the amplitude of ESR signals of bound DSA due to the interaction between ferrocyanide and nitroxide radical of these spin labelled fatty acids observed by Ruf and Gratzl [26], i.e., the largest decrease for 16-DSA, the smallest decrease for 12-DSA and an intermediate decrease for 5-DSA. According to the model of Brown and Shockley model [28], each domain is a double funnel-shaped structure at either end connected by a narrow neck. From the above motional analysis, it would seem that the narrow neck starts at the 5-C of the stearic acid at one end and terminates somewhere between the 13-C and 15-C at the other end; thus the length of the narrow neck can be estimated as 11 ± 1 Å. (see Fig. 9).

Double-hydrogen bonding mechanism

Although it appears that hydrophobic interactions are a major contributions to the binding energy of fatty acids to BSA [3,7,11,28], there is evidence from a variety of methods, including studies of competitive binding with chloride [43], ^{13}C-NMR [17,18] and ESR [21] spectroscopy, and chemical modification studies [12], that electrostatic interactions also play a role. Such interactions might be expected from the pK_α of stearic acid (about 4.8) [38]: it should exist predominantly in anionic form bound to BSA at pH 7.4, thus permitting formation of a salt-bridge type of hydrogen bond with positively charged amino acid side chains.

A comparison of the motional parameters of the DSA and DMS spin labels offers support for the role of hydrogen bonding in the binding of fatty acid to the high-affinity binding sites. Because of the cooperative conformational dynamics of hydrocarbon chains [39], rotation of the nitroxide moiety attached at various chain positions largely reflects rotation of the headgroup. Thus, considering the steric hindrance of the additional methyl group of DMS, one might expect it to exhibit slightly slower rotation than DSA. Experimentally, however, exactly the opposite is observed: the rotation of labeled DMS molecules about the chain axis is significantly faster than that of the analogous DSA molecules.

The discrepancy in $R_\perp$ and $R_\parallel$ values between DSA and DMS admits two possibilities: either that DSA and DMS are bound to different sites on BSA, or that they are bound to similar sites with a different binding mechanism. We cannot entirely rule out the first possibility; however, the $R_\perp$ and $R_\parallel$ values for the two molecules exhibit identical behavior as a function of label position. Also, the A_0 values of spin labels for the two molecules vary in a quite similar way along the hydrocarbon chains, indicating that the magnetic environment of the nitroxide radicals along the two hydrocarbon chains is quite similar, thus suggesting that DSA and DMS do occupy similar binding sites. In our view,

12-DSA, its A_0 value is somewhat larger. In contrast 5-, 7- and 12-DMS have identical A_0 values. This differences can be explained as follows. The caboxyl groups of DSA are hydrated, thus creating a more polar environment around the 5-C nitroxide radical of DSA. However, the methyl carboxylate groups of DMS are hydrophobic, so the polarity of the environment around the 5-C nitroxide radicals of DMS is not affected. Thus, for DMS the 5-C nitroxide radical has the same hydrophobic environment as the 7-C and 12-C nitroxide radicals. Considering the requirements for the surroundings experienced by the 5-C doxyl group in both 5-DSA and 5-DMS, we suggest that 5-C nitroxide radicals are
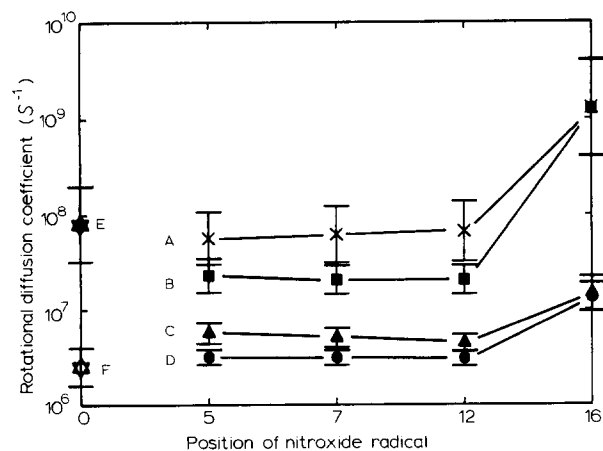

Fig. 7. Plot of rotational diffusion coefficients $R_\perp$, $R_\parallel$ of DSA and DMS bound to BSA in the molar ratio of BSA to spin-labelled stearate of 1:1 vs. position of carbon atom which the nitroxide moiety is attached. (A) $R_\parallel$ values of 5-, 7-, 12- and 16-DMS; (B) $R_\parallel$ values of 5-, 7-, 12 and 16-DSA; (C) $R_\perp$ values of 5-, 7-, 12- and 16-DMS and (D) $R_\perp$ values of 5-, 7-, 12- and 16-DSA. (E) and (F) $R_\parallel$ and $R_\perp$ values obtained by simulation of ESR spectrum of (2,2,6,6-tetramethyl-4-oxyl-piperidine) stearate bound to BSA from Kuznetsov et al. [25].
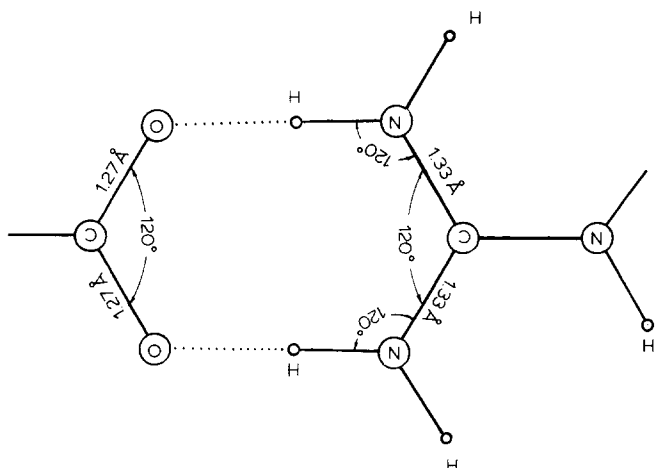
Fig. 8. An illustration of a double-hydrogen bond between a positively charged guanidino group of arginine residue and a negatively charged carboxyl ion of fatty acid. Both the guanidino group and the carboxyl ion are planar, N, H. O atoms involved in the hydrogen bonding are nearly colinear. Due to the ring structure consisting of eight atoms, rotation of fatty acid around either hydrogen bond is hindered. The bond lengths and bond angles are from Refs. 20 and 42.

the second alternative is much more likely, especially given the obvious difference between the headgroups of the two molecules. The negatively charged group of DSA has two oxygen atoms capable of participating in hydrogen bonds. In contrast, the neutral methyl ester of DMS can only form one hydrogen bond. Accordingly, DSA is bound by two hydrogen bonds, so that rotation about either single hydrogen bond is restricted (see Fig. 8). Since DMS cannot form a second hydrogen bond, it remains free to rotate within the binding groove of BSA, leading to the observed increase in $R_\perp$ and $R_\parallel$.

The presence of a double-hydrogen bond can assist in identifying the BSA residue(s) responsible for binding fatty acids. An ideal candidate for this function is arginine, since its guanidino group can form a salt bridge double-hydrogen bond with the carboxylate of the fatty acid (Fig. 8). The resulting ring structure would prevent rotation of the fatty acid chain, as illustrated in Fig. 9. Another possibility is two lysine residues that are located in close proximity to each other, each hydrogen bonded to the carboxylate, such as those in the lysine cluster (532, 534, 536) in the subdomain 3-C, which was assigned as a primary binding site for a long chain fatty acid by Cistola et al. [18].

Our study of the pH dependence of 12-DSA binding was undertaken in an effort to discriminate between arginine and lysine using the difference in the pK_a values of these two side chains [40]. Since we could observe no unbound 12-DSA at low molar ratios of spin probe to BSA, the pH titration was carried out at a molar ratio of 5:1. It proved impossible to study pH values near the pK_a of arginine because of BSA denaturation. However, given the pK_a of lysine (9.8–10.4)
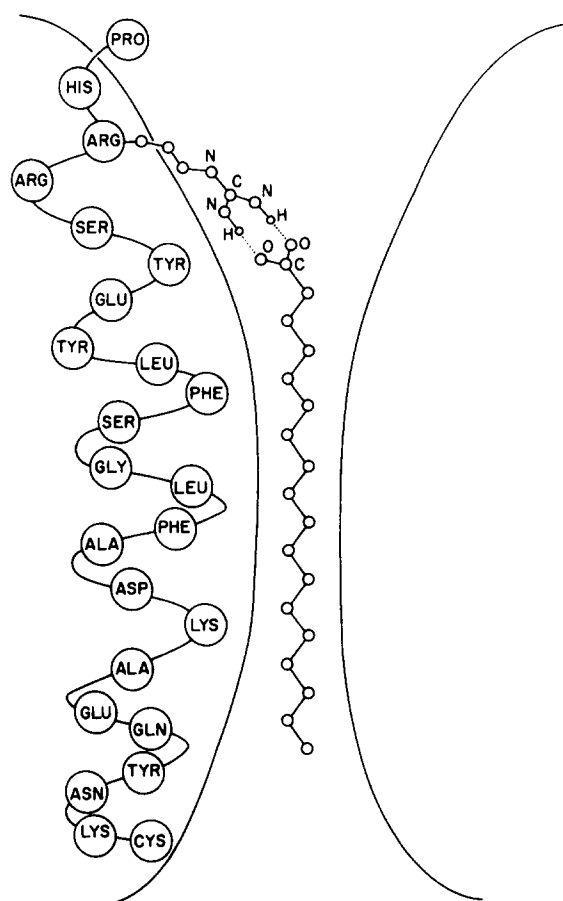

Fig. 9. Schematic diagram of the double-hydrogen bond mechanism of stearic acid binding to BSA. A double-hydrogen bond forms between the negatively charged carboxylate ion and the positively charged guanidino group of residue Arg-335 located at helix 2C-X which consists of six turns, each turn extends 5.4 Å [40]. The length of a stearic acid is 23.8 Å [45]; the length of a side chain of arginine ≈ 6 Å; while the length of the hydrogen bond ≈ 1.6 Å [41]. A stearic acid bound to BSA in this way is just centered at the channel. The channel starts at 5-C of the stearic acid at one end and ends somewhere between 13-C and 15-C. Thus, the length of channel is estimated as 11 ± 1 Å.

[40], one would expect to observe an appreciable decrease of bound 12-DSA in the pH range 10–12 if lysine is participating in hydrogen bonding. As expected from the pK_a values of stearic acid and lysine, the number of bound 12-DSA molecules is practically constant in the pH range 6–9. At pH 11, we observe a sharp decrease in the number of bound 12-DSA molecules, implicating lysine in the binding of stearic acid. Significantly, we observe no decrease at pH 10, indicating that the apparent pK_a of lysine in BSA is shifted above approx. 10.4. This observation is consistent with the ^{13}C-NMR data of the pH dependence of BSA binding of long-chain fatty acids observed by Cistola et al. [18], viz., that long-chain fatty acids (≥ 12 carbon atoms) carboxyl ^{13}C-NMR peaks, which correspond to the three primary long-chain fatty acids binding sites of BSA, exhibited no or only slight change between pH 8.8–11.5. These

^{13}C-NMR data show that the apparent pK_a of the ω-amino group in lysine increases. Also, Cistola et al. observed that in the pH range 3 to 8 these peaks exhibited no change, showing that the apparent pK_a of carboxyl group in fatty acid is lower than 3. The shifts of pK_a of both the ω-amino group in lysine and the carboxyl group in fatty acid provide direct evidence for formation of a salt bridge in the BSA binding of long-chain fatty acids [40,44].

Binding sites of the long-chain fatty acids at the 1-C, 2-C and 3-C subdomains

According to the model of Brown and Shockley, the basic residues located at the mouth of three channels create six long-chain fatty acid binding sites, and subdomains 1-C, 2-C and 3-C correspond to three primary binding sites for long-chain fatty acid [28]. That the number of 12-DSA bound to one BSA decreases to 7 when the pH is increased to 9 in the molar ratio of 12-DSA/BSA of 20 (see Fig. 3) basically agrees with the six high-affinity binding sites for the long-chain fatty acid. There are a total of 22 arginine residues in a BSA molecule. Those which are located at the mouth of the channels are the following seven groups: (10), (81), (143, 144), (193, 195, 197), (334, 335), (411), (434, 443) with parentheses denoting a group. A stearic acid which is hydrogen-bonded to these arginine residues is just centered at the channel as shown schematically in Fig. 9. Thus these seven arginine groups might correspond to the strong binding sites for a long-chain fatty acid, if at least one arginine residue in each of these group is located on the inner face of the channels. The assignment of arginine cluster (143, 144) in subdomain 1-C as a strong binding site is consistent with the inhibition of the reaction of *N*-dansylaziridine (DAZ) at His-145 by stearate, palmitate and oleate [28]. This assignment and the assignment of another arginine cluster (334, 335) in subdomain 2-C, and also the assignment of the lysine cluster (532, 534, 536) in subdomain 3-C agree with the assignments from the ^{13}C-NMR study by Cistola et al. [17,18].

We noticed that among the six high-affinity binding sites, only the one at the right-hand side of domain two * has no arginine residue located at the mouth of the channel. By correlating this distribution of the seven arginine groups with the observation that neither stearate nor palmitate inhibits the interaction of Lys-220 with DAZ and that long-chain fatty acids of 16–18 carbons do not bind at this site until the other four or five long-chain sites are saturated [28], we suggest that arginine residue has a relatively higher affinity for binding long-chain fatty acid than lysine residue.

Conclusion

Nonlinear least-squares fitting of slow-motional ESR simulation to spectra from 5-, 7-, 12- and 16-DSA and 5-, 7-, 12- and 16-DMS bound to BSA gives near rigid limit values of $R_\perp$ and large values of $N = R_\parallel/R_\perp$, indicating that these spin labelled stearates are tightly bound to BSA, and their rotational diffusion around the axis perpendicular to the long molecular axis is greatly hindered. The variation of $R_\perp$, $R_\parallel$ and A_0 from 5-C, 7-C, 12-C to 16-C doxyl radical shows that 7-C and 12-C are trapped in a hydrophobic environment and their motion is hindered, but 16-C is located in a more polar and less hindered environment, whereas 5-C is close to a polar environment, but its motion is still hindered. These analyses suggest that stearic acid and ester stearate are bound to BSA in such a way that they are tightly held in a channel with 5-C located at one end of the channel and the other end of the channel is somewhere between 13-C and 15-C. Therefore, the length of the channel is estimated to be 11 ± 1 Å.

Our contribution to the understanding of the mechanism of BSA binding to fatty acids is as follows. To explain the differences in the values of $R_\perp$ and $R_\parallel$ for stearic acid and ester stearate bound to BSA, a double-hydrogen bond mechanism for binding of long-chain fatty acids was proposed. The double-hydrogen bond (salt bridges) can form either between a positively charged guanidino group in arginine residue and a negatively charged carboxylate ion in fatty acid or between two positively charged ω-amino groups in two closely spaced lysine residues and a negatively charged carboxylate. Due to the ring structure of the double-hydrogen bond, rotation of fatty acid around either hydrogen bond is hindered, and as a result, the fatty acid has a higher rotational barrier around the long hydrocarbon chain than does the ester stearate. The shift of pK_a of the ω-amino group in lysine provides evidence for the formation of a salt bridge in the BSA binding of long-chain fatty acids.

Acknowledgements

References

1 Santos, E.C. and Spector, A.A. (1972) Biochemistry 11, 2299–2302.
2 Morrisett, J.D., Pownall, H.J. and Gotto, A.M., Jr (1975) J. Biol. Chem. 250 2487–2494.

---

* The right-hand side of domains is the side where hinge segments are located.

236

3 Berde, C.B., Hudson, B.S., Simoni, R.D. and Sklar, L.A. (1979) J. Biol. Chem. 254, 391–399.

4 Spector, A.A. and John, K.M. (1968) Arch. Biochem. Biophys. 127, 66–71.

5 Spector, A.A., Fletcher, J.E. and Ashbrook, J.D. (1970) Biochemistry 10, 3229–3232.

6 Spector, A.A., John, K. and Fletcher, J.E. (1969) J. Lipid Res. 10, 56–67.

7 Spector, A.A. (1975) J. Lipid Res. 16, 165–179.

8 Goodman, D.W. (1958) J. Am. Chem. Soc. 80, 3887–3892.

9 Simpson, R.B., Ashbrook, J.D., Santos, E.C. and Spector, A.A. (1974) J. Lipid Res. 15, 415–422.

10 Ashbrook, J.D., Spector, A.A., Santos, E.C. and Fletcher, J.E. (1975) J. Biol. Chem. 250, 2333–2338.

11 Spector, A.A. and Fletcher, J.E. (1977) in Albumin: Structure, Biosynthesis, Function FIBS, 11th meeting Copenhagen Vol. 50, Colloquium B9 (Peters, T. and Sjoholm, I., eds.), pp. 51–60, Pergamon press, Oxford.

12 Jonas, A. and Weber, G. (1971) Biochemistry 10, 1335–1339.

13 Reed, R.G. (1988) Biochim. Biophys. Acta 965, 114–117.

14 Mao, S.Y. and Maki, A.H. (1987) Biochemistry 26, 3576–3582.

15 Oida, T. (1986) J. Biochem. (Tokyo) 100, 1533–1542.

16 Bennett, H.F., Brown, R.D., Koenig, S.H. and Swartz, H.M. (1987) Magn. Reson. Med 4, 93–111.

17 Cistola, D.P., Small, D.M. and Hamiton, J.A. (1987) J. Biol. Chem. 262, 10971–10979.

18 Cistola, D.P., Small, D.M. and Hamiton, J.A. (1987) J. Biol. Chem. 262, 10980–10985.

19 Cistola, D.P. (1985) Biophys. J. 47, 252a–252a.

20 Skar, L.A., Hudson, B.S. and Simoni, R.D. (1977) Biochemistry 16, 5100–5108.

21 Wallach, D.F.H., Verma, S.P., Weidekamm, E. and Bieri, V. (1974) Biochim. Biophys. Acta 356, 68–81.

22 Rehfeld, S.J., Eatough, D.J. and Plachy, W.Z. (1978) J. Lipid Res. 19, 841–849.

23 Soltys, B.J. and Hsia, J.C. (1977) J. Biol. Chem. 253 3023–3028.

24 Soltys, B.J. and Hsia, J.C. (1977) J. Biol. Chem. 253, 3029–3034.

25 Kuznetsov, A.N., Ebert, B., Lassmann, G. and Shapiro, A.B. (1975) Biochim. Biophys. Acta 379, 139–146.

26 Ruf, H.H. and Gratzl, M. (1976) Biochim. Biophys. Acta 446, 134–142.

27 Perkins, R.C., Jr., Abumrad, N., Balasubramanian, K., Dalton, L.R., Beth, A.H., Park, J.H. and Park, C.R. (1982) Biochemistry 21, 4059–4064.

28 Brown, J.R. and Shockley, P. (1982) in Lipid-Protein Interactions (Jost, P.C. and Griffith, O.H., eds.), pp. 25–68 Vol. 1 John Wiley & Sons, New York.

29 Teresi, J.D. and Luck, J.M. (1952) J. Biol. Chem. 194, 823–834.

30 Erlich, R.H., Starkweather, D.K. and Chignell, C.F. (1973) Mol. Pharmacol. 9, 61–73.

31 Moro, G. and Freed, J.H. (1986) The Lanczos Algorithm in Molecular Dynamics: Calculation of Spectral Densities, in Large-Scale Eigenvalue Problems, Mathematical Studies Ser., Vol. 127 (J. Cullum and R. Willoughby, eds), North-Holland, Amsterdam.

32 Moro, G. and Freed, J.H. (1981) J. Chem. Phys. 74, 3757–3773.

33 Harrington, W.F., Johnson, P. and Ottewill, R.H. (1975) Biochem. J. 15, 137–141.

34 Free, J.H. (1964) J. Chem. Phys. 41, 2077–2087.

35 Moser, P., Squire, P.G. and O'Konski., C.T. (1966) J. Phys. Chem. 70, 744–755.

36 Wright, A.K. and Thompson, M.R. (1975) Biophys. J. 15, 137–141.

37 Gaffney, B.J. and McConnell, H.M. (1974) J. Magn. Res. 16, 1–28.

38 Lyman, W.J., Roehl, W.F. and Rosenblatt, D.H. (1982) in Handbook of Chemical Property Estimation Methods Environment Behavior of Organic Compounds pp. 6.1–6.28, McGraw-Hill, New York.

39 Ferrarini A., Nordio, P.L., Moro, G.J., Crepeau, R.H. and Freed, J.H., (1989) J. Chem. Phys. 91, 5707–5721.

40 Cantor, C.R. and Schimmel, P.R. (1980) Biophysical Chemistry Part 1, pp. 50, W.H. Freeman, San Francisco.

41 Johnson, M.E. (1981) Biochemistry 20, 3319–3328.

42 CRC Handbook of Biochemistry and Molecular Biology (1975), 3rd Edn. Physical and chemical data, (Fasman, G.D., ed.), Vol. 2, pp. 222.

43 Saroff, A. (1957) J. Phys. Chem. 61, 1364–1368.

44 Fersht, A.R. (1971) J. Mol. Biol. 64, 497–509.

45 Wibant, J.P. (1951) Organic Chemistry translated from 16th Dutch edition by Sammuel Coffer, D. Sc. (Leyden), pp. 71, F.R.I.C. Elsevier, Amsterdam.

46 Crepeau, R.H., Rananavare, S., and Freed, J.H., (1987) Abstracts of the 10th international EPR symposium, Rocky Mountain confrence, Denver, CO.